Advances in Science and Technology Research Journal

Advances in Science and Technology Research Journal, 2027, 21(1), 1–13
https://doi.org/10.12913/22998624/226553
ISSN 2299-8624, License CC-BY 4.0

Received: 2026.07.02
Accepted: 2026.11.15
Published: 2026.12.01

Influence of pulse laser treatment parameters on the microstructure and surface properties of Ti-6Al-4V alloy

Magdalena Jażdżewska[1*], Mieszko Jarzębowski[1], Andrzej Szczypior[1], Natalia Jowsa[1], Julia Ellwart[1], Karolina Grabowska[1], Michał Mozol[1], Marta Kaczorowska[1]

[1] Faculty of Mechanical Engineering and Ship Technology, Gdańsk University of Technology, 80-233 Gdańsk, Poland
* Corresponding author's e-mail: magdalena.jazdzewska@pg.edu.pl

ABSTRACT

Titanium and its alloys are nowadays broadly used in medical and advanced technical applications. Besides their corrosion resistance, lightweight, and durability, they exhibit relatively low hardness and wear resistance, as well as only weak bioactivity. Among the particularly promising titanium materials, Ti-6Al-4V alloy is still the most widely applied in implantology. In the present research, this Ti alloy was subjected to mechanical grinding followed by laser irradiation with varying parameters, such as pulse laser power, pulse frequency, and scan rate. The topography determined by roughness and waviness, hydrophilicity determined by water contact angle, microhardness on the surface and within the created remelted surface layer, and corrosion resistance were determined. The roughness, waviness, and microhardness became greater with increasing scan rates, 7.5 mm/s and more. The water contact angle was scarcely affected by laser modification parameters, remaining close to 85º. Corrosion resistance improved after laser irradiation, regardless of the laser parameters. When analyzing all applied laser treatment parameters and obtained results, it can be concluded that the most convenient modified surface can be achieved for Ti-6Al-4V alloy at a laser power of 2000 W, a frequency of 25 Hz, and a scan rate of 7.5 mm/s. This positive result can be attributed to the melting and remelting processes occurring within the thin surface layer, substantially related to the delivered thermal energy, maximum temperature, diffusion, and rapid solidification of the layer.

Keywords: Ti-6Al-4V alloy, laser treatment, surface properties, wettability, hardness, roughness.

INTRODUCTION

Titanium and its alloys belong to the most important engineering and biomedical materials due to their favorable combination of low density, high specific strength, excellent corrosion resistance, and good biocompatibility [1–3]. Among them, the Ti–6Al–4V alloy is by far the most widely used, finding applications in aerospace, motorsport, and medical implantology, particularly for load-bearing implants such as hip stems, dental implants, and fixation devices [4–7]. Despite these advantages, Ti–6Al–4V still exhibits several limitations, including relatively low surface hardness, poor wear resistance, and suboptimal surface characteristics for long-term tribological and biological performance [8,9].

In many advanced applications, especially in implantology, the surface properties of a material are often more critical than its bulk characteristics. Parameters such as surface roughness, waviness, wettability, and near-surface hardness strongly influence wear behavior, osteointegration, and mechanical stability [10–12]. Consequently, significant research effort has been devoted to developing the surface modification techniques that enhance the functional performance of titanium alloys without compromising their favorable bulk properties.

Various surface engineering methods have been proposed for the Ti–6Al–4V alloy, including

chemical treatments, anodization, plasma spraying, ion implantation, and mechanical surface treatments [13–17]. While many of these techniques can improve selected surface properties, they often suffer from drawbacks such as limited layer adhesion, environmental concerns, complex processing routes, or insufficient control over microstructural features. In this context, laser surface modification has emerged as a promising alternative, offering high precision, localized energy input, as well as the ability to tailor surface morphology and microstructure through controlled processing parameters [18–20].

Laser surface melting, in particular, enables rapid heating and cooling of the surface layer, leading to microstructural refinement, increased hardness, and the formation of characteristic surface patterns [21–23]. However, the effects of laser processing are highly sensitive to parameters such as laser power, pulse frequency, and beam scanning velocity. The literature reports diverging observations regarding the influence of these parameters on surface roughness, wettability, and hardness, especially for pulsed Nd: YAG laser systems [24–27]. Some studies report enhanced hydrophilicity after laser treatment, while others observe a transition toward hydrophobic behavior, depending on the resulting surface topography and oxidation state [28,29]. These discrepancies highlight the need for systematic studies that simultaneously correlate laser parameters with multiple surface characteristics.

Despite extensive research, there remains a lack of consensus on the optimal laser processing conditions that provide a balanced improvement in the tribological and mechanical properties of Ti–6Al–4V surfaces, particularly for applications requiring controlled roughness and increased near-surface hardness. Moreover, comparative studies combining optical microscopy, wettability analysis, surface topography measurements, and microhardness evaluation under identical processing conditions are still limited.

Therefore, the present study aimed to systematically investigate the influence of selected pulsed laser surface modification parameters – namely laser power, pulse frequency, and beam moving velocity – on the surface layer properties of Ti–6Al–4V alloy. The surface morphology, wettability, waviness, roughness, and microhardness of laser-treated samples were analyzed and compared to those of the untreated reference material. Based on the obtained results, an optimal set of laser processing parameters was identified, providing enhanced surface characteristics suitable for medical implants as well as advanced technical applications in aerospace and motorsport industries.

MATERIALS AND METHODS

Material

For this research, fifteen samples of the Ti-6Al-4V alloy were cut from the bar made of the mentioned alloy. Each of them has a diameter of 14 mm and a height of 3 mm. Surfaces on both sides of the samples were ground using sandpaper with progressively finer grades, ending at grade 800. The material prepared in this way was ready for laser treatment.

Laser treatment

Before remelting, the surface was cleaned with isopropyl alcohol. Laser surface treatment was carried out using a TRUMPF TruLaser Station 5004 workstation equipped with a TRUMPF TruPulse 156 pulsed Nd:YAG laser operating at a wavelength of 1064 nm. The laser beam generated by the laser source was transmitted to the processing head through the optical beam delivery system and focused onto the specimen surface, resulting in a laser spot diameter of approximately 1 mm. The specimens were mounted on the worktable, while the predefined scanning paths were generated by the CNC-controlled movement of the laser processing head. High-purity argon (Argon 6.0, Linde) was continuously supplied through a coaxial shielding nozzle at a constant pressure of 3.5 bar to protect the molten pool from atmospheric contamination during laser irradiation. The pulse duration was kept constant at 1 ms, whereas the laser power, pulse repetition frequency, and beam scanning velocity were varied according to the experimental design. The laser power ranged from 1500 to 2500 W, the pulse repetition frequency was 10 or 25 Hz, and the beam scanning velocity varied between 2.3 and 10 mm/s. The processing parameters are summarized in Table 1. Sample code was created as a: power value [kW], frequency value [Hz], velocity value [mm/s]. After laser treatment, samples were naturally cooled in the atmospheric air.

Optical (light) microscopy

The first surface examinations were made using an optical microscope BX 51 (Olympus, Tokyo, Japan). The microstructure was observed at magnification from 50x to 1000 times.

Wettability

Wettability of the modified surfaces was investigated using the sessile drop method and determined as water contact angle (WCA). Ultrapure distilled water was used as the test liquid. The measurements were performed with an Attension Theta Life goniometer (Biolin Scientific, Espoo, Finland). The droplet volume was approximately 2 µL, and the contact angle was recorded 10 s after the droplet deposition on the sample surface.

Waviness and roughness

After analyzing the images from the optical microscope and the results of contact angle measurements (WCA), five samples were chosen to measure the wettability and roughness research. The WCA measurements were made with the Hommel-Etamic waveline profilometer by Jenoptik. Because of the path that followed the laser beam during modification, the needle of the profilometer slid along a straight line, perpendicular to the pattern on the samples. This allowed analyzing the waviness and roughness parameters on the whole surface rather than in the one line created by a moving laser beam. It allowed determining a couple of roughness parameters (Ra_{10}, Rz_{10}, Rp_{10}, Rt) and waviness Wt.

Microhardness of the surface

The tests were performed using the Vickers method with two different loads: 100 gf (HV0.1) and 25 gf (HV0.025). The application of different loads allowed evaluation of hardness changes at various indentation depths, providing insight into the mechanical response of the near-surface region. Each load was applied three times in slightly different locations on the sample's surface. The microhardness measurements were carried out using a Future Tech FM-ARS-F Automatic Micro Hardness Tester.

Microhardness of the cross-section

All previously investigated samples were cut vertically in half and then included in resin. Connecting a few samples in one holder (two in one and three in another one) significantly sped up their further preparation. That preparation included polishing and etching the surface of the titanium alloy with Kroll's reagent (a few times for approximately 5 seconds each). This allowed seeing the differences between grains

Table 1. Different parameters of laser modification

Sample number	Sample code	Power [W]	Frequency [Hz]	Velocity [mm/s]
1	1.50–10–5.0	1500	10	5
2	1.75–10–5.0	1750	10	5
3	2.00–10–5.0	2000	10	5
4	2.25–10–5.0	2250	10	5
5	2.50–10–5.0	2500	10	5
6	1.50–10–10.0	1500	10	10
7	1.75–25–2.3	1750	25	2.3
8	1.75–25–10.0	1750	25	10
9	2.00–25–10.0	2000	25	10
10	2.25–25–10.0	2250	25	10
11	2.50–25–10.0	2500	25	10
12	1.50–25–7.5	1500	25	7.5
13	2.00–25–7.5	2000	25	7.5
14	2.25–25–7.5	2250	25	7.5
15	2.50–25–7.5	2500	25	7.5

across the material. For these investigations, the same equipment (microhardness tester and optical microscope) was used as in the previously mentioned analysis. The microhardness measurements were conducted on the cross-section of every prepared sample.

Corrosion tests

The following samples were used for the corrosion test: 1.50–10–5.0, 2.50–10–5.0, 1.75–25–2.3, 1.75–25–10, and 1.50–25–7.5. The setup consisted of an auxiliary electrode (CE) – a platinum electrode, a reference electrode (RE) – a calomel electrode, and a working electrode (WE) – the tested sample. During the experiment, each sample was immersed in 200 mL of Ringer's solution. The solution was continuously heated to maintain a constant temperature of 37 °C, corresponding to the conditions similar to those in the human body. A potentiostat (Atlas 0531, Atlas Sollich, Poland) with additional AtlasCorr05 software was used for the measurements, allowing the determination of the corrosion potential (E_{corr}) and corrosion current density (I_{corr}) [28–30].

RESULTS

Topography

The samples modified with a velocity of 5 mm/s and frequency 10 Hz had a regular wavy pattern on their surfaces. Each of the waves covers the next in approximately 30%, and their edges are relatively far from each other (Figure1a). Sample 1.50–10–10.0 was also modified with frequency 10 Hz, but a velocity equal to 10mm/s created many separated craters at the surface, rather than a smooth melted wavy structure (Figure 1b). Because of that, other samples were treated with a higher frequency equal to 25 Hz. Using this parameter with different powers and velocities of the laser beam, getting a smooth wavy pattern was possible again. With this frequency, the edges of the waves are closer to each other. On sample 1.75–25–2.3, on which the laser beam velocity was set as 2.3 mm/s, the waves are the thinnest (Figure 1c). On the samples modified with higher velocity, waves overlap one another in approximately 50% (Figure 1d). In the

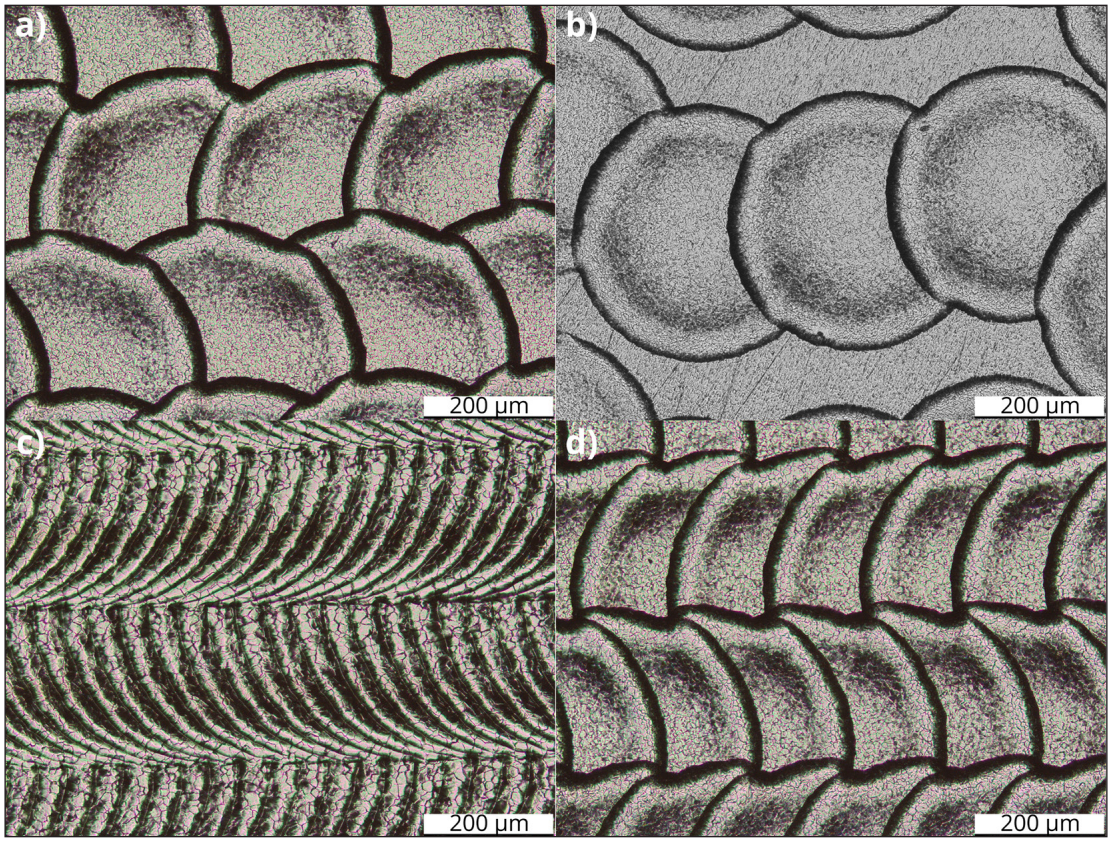


Figure 1. Surfaces of the samples after laser treatment: a) 1.75–10–5.0, b) 1.50–10–10.0, c) 1.75–25–2.3, d) 1.50–25–7.5

microstructure of three samples (2.00–25–7.5, 2.25–25–7.5, 2.50–25–7.5), oxidation was recognized, especially at the edges of the samples. It is seen as a change of color from metallic silver to golden and multi-colored (Figure 2).

Wettability

For each sample, three measurements were carried out, with the water droplet placed at different locations to account for possible surface heterogeneity. The untreated surface was used as the reference value (sample 0). The results are presented as mean contact angle values along with their standard deviations and are summarized in Table 2.

The contact angle measured for the untreated reference sample (sample 0) was approximately 62°, indicating relatively good wettability of the surface. After laser treatment, a significant increase in the contact angle was observed for all modified samples, with values ranging from about 78° to 99°, which corresponds to reduced wettability and a more hydrophobic surface character. The highest mean contact angle was obtained for sample 1.50–10–5.0, reaching approximately 99°. For the remaining samples, the contact angle values varied depending on the applied laser parameters, but in most cases were in the range of 80–90°.

Based on the obtained results, no clear relationship between the contact angle values and the individual laser processing parameters, such as laser power, pulse frequency, or scanning velocity, was observed. Although differences in the contact angle were noted among the samples, the variations did not exhibit a monotonic trend with respect to any of the investigated parameters. At the same time, all laser-treated samples showed higher contact angle values compared to the reference sample, indicating that laser surface modification leads to an overall reduction in surface wettability.

Waviness and roughness

Table 3 shows the results from the analysis of chosen samples. The surface of every analyzed sample was much rougher and wavier than before modification. Material without laser treatment (grained with 800-grit sandpaper) had waviness at the level of 2 µm, while in modified surfaces this parameter was a few times higher. Also, roughness increased significantly, which is easy to spot in every one of the roughness parameters. Theoretically, sample 2.50–25–10.0 had the most deformed surface, but a very high standard deviation prevented the authors from treating it as a reliable result. Regardless of the analyzed parameter, it is sure that laser treatment developed the surface of Ti-6Al-4V alloy to the desired level in medical applications [27].

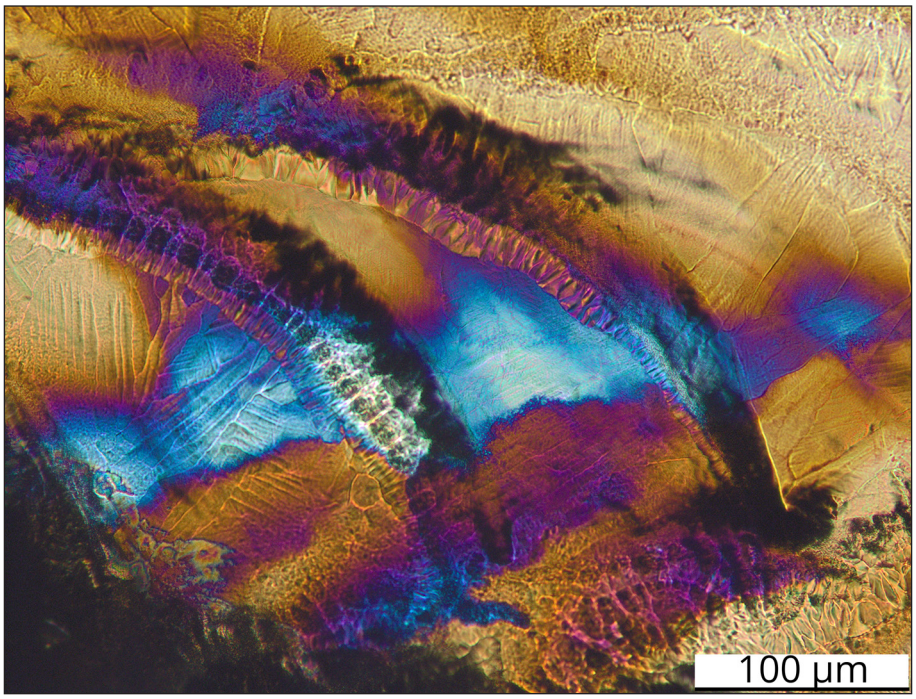


Figure 2. Surface of sample 2.25–25–7.5 after laser treatment, with visible oxidized fragment

Table 2. Water contact angle values at different laser irradiation parameters

Sample code	Mean contact angle [°] ± SD
0 (reference)	62.17 ± 3
1.50–10–5.0	99.04 ± 4
1.75–10–5.0	89.89 ± 1
2.00–10–5.0	82.01 ± 10
2.25–10–5.0	85.23 ± 7
2.50–10–5.0	87.31 ± 1
1.50–10–10.0	80.28 ± 7
1.75–25–2.3	80.66 ± 9
1.75–25–10.0	83.73 ± 8
2.00–25–10.0	85.16 ± 6
2.25–25–10.0	81.81 ± 4
2.50–25–10.0	78.28 ± 3
1.50–25–7.5	84.07 ± 2
2.00–25–7.5	81.81 ± 4
2.25–25–7.5	81.54 ± 9
2.50–25–7.5	87.74 ± 4

Microhardness of the surface

Results are presented in Tables 4 and 5. The microhardness measurements confirmed that laser surface modification increased the hardness of the Ti-6Al-4V alloy in the near-surface region. For the low indentation load of 25 gf (HV0.025), a clear increase in hardness was observed in comparison with the non-modified surface. The microhardness rose from approximately 271 HV for the reference sample to about 314–353 HV for the laser-treated and reference samples, consistent with the expected effect of laser surface modification. Although the microhardness differences between the laser-modified samples are small and difficult to clearly distinguish, partly due to relatively large standard deviations, the highest average value (approximately 353 HV) was recorded for sample 2.00–25–7.5.

In contrast, measurements at a higher load of 100 gf (HV0.1) did not show a distinct difference in hardness between the laser-treated and reference samples. This is attributed to the deeper penetration of the indenter, which exceeded the thickness of the laser-modified layer, resulting in the measured hardness being influenced by the softer substrate.

The microhardness study confirms that an increase in hardness induced by laser processing is limited to the surface and subsurface regions.

Microhardness of the cross-section

Due to the uncertain results of the microhardness analysis on the surface, it was decided to research the cross-section of the material. The results of this analysis are shown in Figure 3. Investigation of the microstructure allowed for the measurement of the thickness of each layer at the cross-section of the samples.

As seen in Figure 3, most samples near their surface had a hardness greater than 350 HV. The exception was sample 1.50–10–10.0, but it had many separated craters rather than a fully melted surface, which resulted in measuring unmodified alloy. The hardness was usually high near the surface and then decreased, approaching the center of the sample. The subsurface area of all samples had the lowest hardness, significantly lower than the value on the surface. In the center of the samples, values of hardness were (surprisingly) getting high again. In some cases, like 1.75–10–5.0 or 2.50–25–10, the inside layers were even harder than laser-modified surfaces. Nevertheless, analysis showed that with specific parameters (power 2000 W, frequency 25 Hz, and velocity 7.5 mm/s) it is possible to reach a hard surface of the material.

Analyzing images from an optical microscope, with a magnification of 200, allowed describing the thickness of every layer. Differences in grain structure were seen just after etching the surface of cross sections with Kroll's

Table 3. Waviness and roughness parameters of some tested specimens

Sample code	Wt [µm]	Ra_{10} [µm]	Rz_{10} [µm]	Rp_{10} [µm]	Rt [µm]
0 (reference)	2.137 ± 0	0.087 ± 0	0.710 ± 0	0.417 ± 0	1.133 ± 0
1.75–10–5.0	9.223 ± 1	2.853 ± 0	10.530 ± 0	6.130 ± 0	12.960 ± 0
1.50–10–10.0	7.213 ± 2	1.720 ± 0	6.237 ± 1	4.040 ± 0	7.557 ± 1
2.25–25–10.0	9.223 ± 0	3.907 ± 0	16.060 ± 0	7.450 ± 0	20.463 ± 1
2.50–25–10.0	18.260 ± 10	4.353 ± 0	17.570 ± 0	7.610 ± 0	23.180 ± 4
2.00–25–7.5	6.673 ± 1	3.110 ± 1	12.510 ± 1	6.807 ± 1	15.400 ± 1

Table 4. Microhardness measured at 100 gf

Sample code	HV0.1 (100 gf) ± SD	HRC ± SD
0 (reference)	306 ± 7	30.81 ± 1
1.75–10–5.0	323 ± 28	32.52 ± 3
1.50–10–10.0	288 ± 11	28.23 ± 1
2.25–25–10.0	299 ± 27	29.64 ± 3
2.50–25–10.0	311 ± 3	31.22 ± 0
2.00–25–7.5	311 ± 20	31.09 ± 2

Table 5. Microhardness measured at 25 gf

Sample code	HV0.025 (25 gf) ± SD	HRC ± SD
0 (reference)	271 ± 21	24.89 ± 3
1.75–10–5.0	314 ± 14	31.50 ± 2
1.50–10–10.0	319 ± 17	32.16 ± 2
2.25–25–10.0	329 ± 15	33.31 ± 2
2.50–25–10.0	314 ± 33	31.43 ± 4
2.00–25–7.5	353 ± 16	35.92 ± 2

reagent. It showed that the melted material had a thickness that varies from 20 to even 80 µm, depending on the place (peak or valley), as seen in Figure 4. Values presented there are mean values from ten measurements, performed at each of the cross section. The medium value of the outer layer thickness also depended on the parameters of modification. The higher laser power (2250 and 2500 W) allowed for the greatest thickness and the highest waves on the surface. Subsurface area, which visually differs from other layers of the cross-section, ranged from 40 to 60 µm on every sample. Below the subsurface layer, material was unchanged.

Corrosion tests analysis

A decrease in the corrosion current density and an increase in the corrosion potential improve the corrosion resistance of the material. In Table 6, for each of the tested samples, an increase in the corrosion potential and a decrease in the corrosion current density can be observed.

From the curves in Figure 5a, the laser-treated samples exhibit a higher corrosion potential than the base-material sample. This indicates that they had greater corrosion resistance. The 1.75–25–2.3 sample achieved the most stable potential. The most negative initial potential gradually shifted toward more positive values, which indicates slow repassivation and the presence of a less stable oxide layer. Figure 5b shows, for all samples, a shift toward more positive values compared to the reference sample. The most favorable laser processing parameters were observed for the following samples: 1.75–25–2.3; 1.75–25–10; and 1.50–25–7.5.

DISCUSSION

Surface morphology

The use of a pulsed laser for surface irradiation results in an irreversible change within the surface layer as a consequence of its heating, melting, evaporation, and plasma formation. The experimental results reported by several review papers [34-37] confirm earlier findings that laser surface modification is an effective method for tailoring the properties of Ti-6Al-4V alloy. The

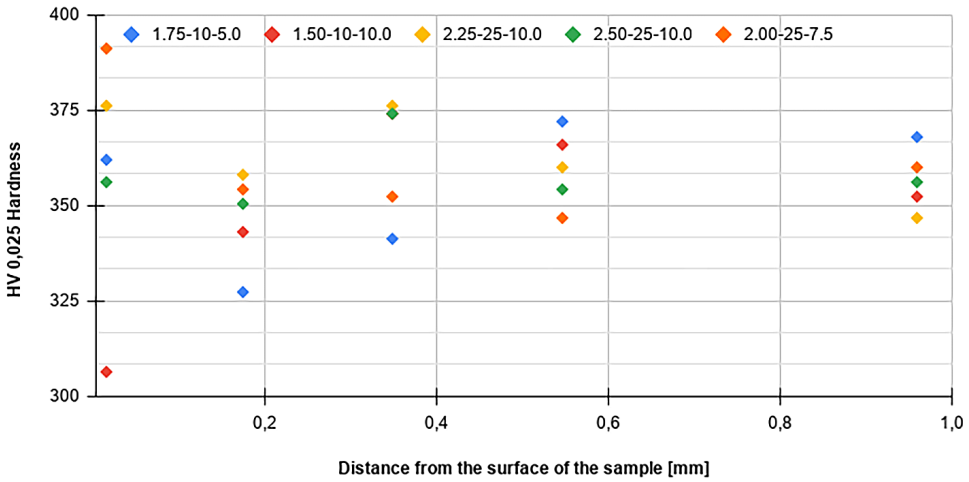


Figure 3. Hardness dependence on the distance from the surface of the sample measured on cross-sections

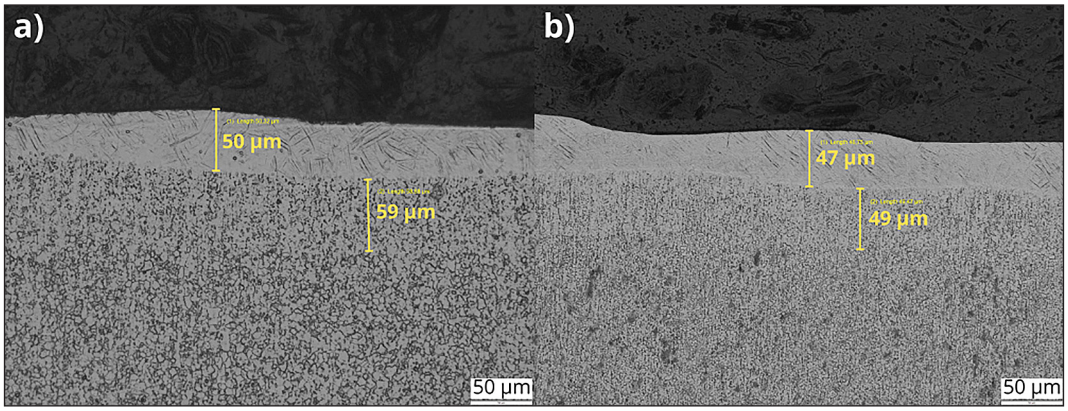


Figure 4. Cross sections of the samples: a) 1.75–10–5.0, b) 2.50–25–10

Table 6. Corrosion potential and corrosion current density

Sample code	E_{corr} (V)	I_{corr} (A/cm^2)
0 (reference)	-3.91 × 10^{-1}	7.91 × 10^{-7}
1.50–10–5.0	-3,61 × 10^{-1}	0.11 × 10^{-7}
2.50–10–5.0	-1.79 × 10^{-1}	1.00 × 10^{-7}
1.75–25–2.3	-1.59 × 10^{-1}	1.06 × 10^{-7}
1.75–25–10	-2.36 × 10^{-1}	0.93 × 10^{-7}
1.50–25–7.5	-2.41 × 10^{-1}	0.89 × 10^{-7}

surface topography is highly sensitive to the balance between pulse frequency and beam moving velocity (scan rate), i.e., the laser energy density. The origin of observed surface topography properties was attributed to cumulative exposure and enhanced local energy absorption at the overlap regions [38]. Specifically, at a low frequency of 10 Hz and a higher beam velocity (10 mm/s), the laser irradiation results in the formation of isolated craters, rather than a continuous melt pool. In contrast, increasing the frequency to 25 Hz allows for a stable overlap of approximately 50%, leading to a continuous and regular wavy pattern. Such a behavior can be related to the effects of the high speed and energy of the laser irradiation, resulting in high rates of heating and solidification and the appearance of a needle-like non-equilibrium martensitic α' phase [39]. In [40], the laser treatment caused an expansion of the heat-affected zone with increasing laser pulse frequency. As reported in [41], at laser fluence of 70 J/cm^2, the relatively shallow and uniform grooves structures appeared, at 110 J/cm^2, the microdroplets, molten splatters, and flat pits were present together with an expansion of the heat affected zone significantly, at 140 J/cm^{2,} numerous grooves and ridges created a highly porous network, and finally at 180 J/cm^2, a transition occurred and the grooves were no longer observed. The laser beam shape was also important [42], as the Gaussian beam brought out positive changes in microstructure at ≤130 J/mm^3, but increased the surface roughness and porosity at h ≥150 J/mm^3. In contrast, the irradiation with the ring-based beam resulted in higher porosity at low fluence and in high density and smoother surfaces at high fluence. The porosity after laser treatment was observed in the form of nano- and sub-micro-sized pores [43]. The effects were also dependent on the media in which irradiation was performed [44], with the preferred sodium nitrate solution and worse results for hydrogen peroxide and sodium bicarbonate. The obtained results indicate that by changing the frequency, it is possible to create different large-scale surface images with a simultaneous presence of smoothness at the microscale. The complexity of the processes occurring during irradiation forces us to search for the best combination of all the parameters studied here, such as laser power, frequency, and scan rate.

Roughness

This laser-enhanced structural development is directly and intensively reflected in the roughness parameters; for instance, the Ra_{10} value increased from 0.087 µm for the reference material to values exceeding 4 µm for the laser-modified samples. This result is comparable to several earlier investigations made on Ti-6Al-4V alloy [45]. In [38], for the same alloy, after DLIP, the average roughness was 8.5 ± 0.5 µm, and in [46], for Ti-6Al-4V and Ti-13Zr-13Nb alloys, the Ra was 2.89 and 5.40 µm. However, in [47], the roughness values after laser processing were between 50 and

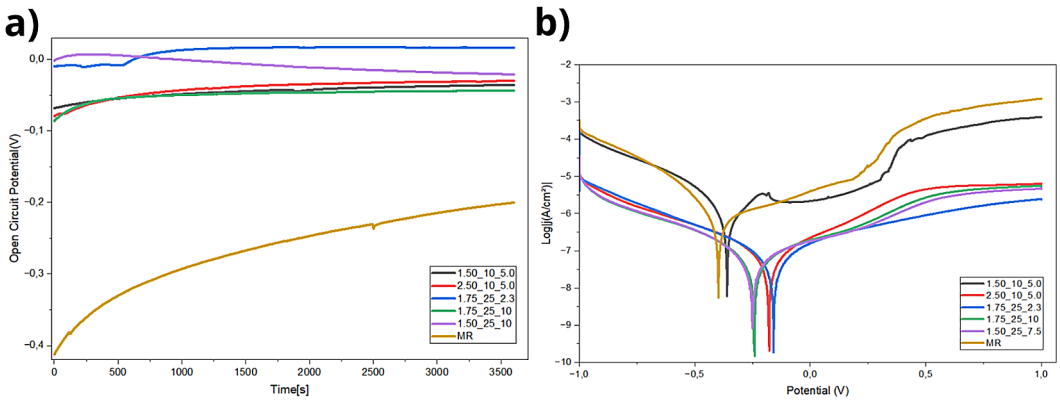


Figure 5. a) Open-circuit potential vs. time, b) potentiodynamic corrosion curves

88 um for Ra, and between 48 and 93 um for Sa, quite large values as compared to about 6 um for the non-treated alloy. The excessive roughness observed after laser treatment or for SLM-made titanium can be diminished by different processes, such as chemical post-processing (acid etching), resulting additionally in an improvement of fatigue strength [48], or the finish turning process under dry or MQL (minimum quantity lubrication) machining [49]. The moderate roughness developed here is considered advantageous for medical applications, as it promotes better adhesion of osteoblasts and bone ingrowth.

Wettability

The water contact angle measurements revealed a significant but limited change in wettability related to the laser treatment parameters. The untreated reference material showed a contact angle of 62.17°. Following laser modification, the surface became nearly hydrophobic, with contact angles exceeding 85° and reaching up to 99° for specific parameters. Such behavior is in opposition to an earlier report on laser-treated Ti-6Al-4V alloy [50]. However, as shown in several investigations [45], the laser treatment can be successfully applied to obtain both hydrophilic and even superhydrophobic titanium surfaces. In [38], the laser treatment of Ti-6Al-4V substrates led to the appearance of high water contact angles with the rose petal wetting regime. In another research [41], the superhydrophilic nature and moderate hydrophilic condition with contact angles from 40º to 60º was observed for lower fluence, and superhydrophobic behavior for higher fluence. On the contrary, in [47], the water contact angle was always 65 and 80º, independently of the process parameters. Low hydrophilicity or hydrophobicity is undesired when considering the surface's ability to integrate with biological cells. Further biological in vivo tests will focus on investigations of how these two potentially opposite effects, increasing roughness and lowered hydrophilicity, will positively or negatively affect bioactivity and cytotoxicity, i.e., adhesion of osteoblasts and adhesion of bacteria. Presumably, identifying intermediate laser irradiation parameters will be the prime objective. It should be noted that the laser surface modification can result in both hydrophilic and hydrophobic surfaces.

Microhardness

Mechanical testing via the Vickers method confirmed that the hardening effect is primarily localized in the surface area. At low indentation load (HV0.025), a clear increase in microhardness was observed, rising from 271 ± 21 HV for the reference sample to a maximum average of 353 ± 16 HV for sample 2.00-25-7.5. This represents a hardening of approximately 30%. However, the lack of significant hardness changes at higher loads (HV0.1) confirms that the modified layer is relatively thin, as the indenter reached the softer substrate material. Further investigations, with a cross-section of samples, confirmed that laser-treated material has the highest value of hardness. It also allowed measuring the thickness of modified layers, which vary from 20 to 80 µm. The increasing hardness following the laser treatment was quite frequently observed, as shown in [45,51]. In particular, in [46] the highest value observed for the irradiated Ti-13Nb-13Zr alloy was of 5.18 GPa, in [52] the peak hardness reached 412 HV, corresponding to an increase of

about 21% compared to the untreated metal, with the hardened layer of ~400 μm, and in [53] the hardness ranged between 310 and 526 HV, with its value increasing with laser pulse intensity and pulse frequency. The mechanism of surface layer hardening can be related to periodic ripple structures created by remelting and solidifying [54], the refinement of the microstructure and the formation of α′ martensite [55,56], and the transformation of the coarsened alpha phase grains into elongated ones, increasing the grain boundary length [57].

Corrosion

Measurements of corrosion potential and corrosion current density indicate that the titanium alloy with aluminum and vanadium, after laser modification, is much less susceptible to corrosion. The increase in corrosion resistance was attributed in the past to different phenomena such as the creation of periodic topography, better passivity, low fraction of high-angle grain boundaries, or a change in α/β phase ratio [45,58]. Previously, in [53], the corrosion potential of laser-treated surfaces was nobler in comparison to unprocessed Ti-6Al-4V alloy, and became more positive with increasing laser intensity and pulse densities, together with decreased corrosion rates due to the microstructure refinement. It is greatly important to achieve high corrosion resistance when considering the long-term behavior of an implant in the body.

CONCLUSIONS

In this research, the influence of several laser processing parameters on the properties of Ti-6Al-4V alloy surfaces was investigated. The research demonstrated that laser treatment effectively modifies the surface topography, creating a more developed and deformed structure compared to the untreated material. Some surface properties, such as microhardness, wettability, and corrosion resistance, were related to the process parameters.

To ensure uniform melting of the surface, a higher laser beam scan rate is desired, requiring simultaneously a correspondingly increased pulse frequency to maintain a stable pattern. Roughness is increased to an acceptable level by increasing all the laser power, frequency, and scan rate so that with the energy density.

The microhardness is significantly increased within the heat-affected zone of 20–80 μm compared to the untreated alloy. The process parameters scarcely affect the microhardness, likely due to similar energy density.

The wettability of the processed material is significantly reduced, as the modified samples exhibit a nearly hydrophobic character. As for microhardness, no process variable substantially changed the water contact angle by more than the standard deviation.

The laser modification leads to an increase in corrosion resistance (decrease in corrosion current density) of Ti-6Al-4V alloy in Ringer's solution by about an order of magnitude. The lowest corrosion current values were observed for the surface treated with the lowest pulse energy, frequency, and scan rate. Supposedly, the higher energy densities resulted in a more inhomogeneous surface, as the number of corrosion microcells is considered.

Ultimately, an optimal set of laser power of 2000 W, frequency of 25 Hz, and beam moving velocity of 7.5 mm/s was identified to enhance the surface properties of Ti-6Al-4V alloy for advanced medical and technical applications.

Acknowledgments

The authors would like to thank the employees of Gdańsk University of Technology: M. Czajkowski, G. Gajowiec, D.B. Kwidzińska, R. Jesiołkiewicz, and J. Sypniewska for their technical assistance in some of the analyses. The authors also thank their colleague K. Wolska for exchanging experiences about the team research project.

REFERENCES

1. Niinomi M. Mechanical properties of biomedical titanium alloys. Mater. Sci. Eng. A 1998, 243, 231–236, https://doi.org/10.1016/S0921-5093(97)00806-X
2. Long M.; Rack H.J. Titanium alloys in total joint replacement—A materials science perspective. Biomaterials 1998, 19, 1621–1639, https://doi.org/10.1016/S0142-9612(97)00146-4
3. Elias C.N.; Lima J.H.C.; Valiev R.; Meyers M.A. Biomedical applications of titanium and its alloys. JOM 2008, 60, 46–49, https://doi.org/10.1007/s11837-008-0031-1
4. Boyer R.; Welsch G.; Collings E.W. Materials Properties Handbook: Titanium Alloys; ASM International: Materials Park, OH, USA, 1994.
5. Geetha M.; Singh A.K.; Asokamani R.; Gogia A.K. Ti-based biomaterials, the ultimate choice

for orthopaedic implants—A review. Prog. Mater. Sci. 2009, 54, 397–425, https://doi.org/10.1016/j.pmatsci.2008.06.004

6. Leyens C.; Peters M. Titanium and Titanium Alloys: Fundamentals and Applications; Wiley-VCH: Weinheim, Germany, 2003, https://doi.org/10.1002/3527602119
7. Kaur M.; Singh K. Review on titanium and titanium based alloys as biomaterials for orthopaedic applications. Materials Science and Engineering: C, September 2019, 102, 844–862, https://doi.org/10.1016/j.msec.2019.04.064
8. Donachie M.J. Titanium: A Technical Guide, 2nd ed.; ASM International: Materials Park, OH, USA, 2000.
9. Budinski K.G. Tribological properties of titanium alloys. Wear 1991, 151, 203–217, https://doi.org/10.1016/0043-1648(91)90249-T
10. Wennerberg A.; Albrektsson T. Effects of titanium surface topography on bone integration: A systematic review. Clin. Oral Implants Res. 2009, 20, 172–184, https://doi.org/10.1111/j.1600-0501.2009.01775.x
11. Buser D.; Schenk R.K.; Steinemann S.; Fiorellini J.P.; Fox C.H.; Stich H. Influence of surface characteristics on bone integration of titanium implants. J. Biomed. Mater. Res. 1991, 25, 889–902, https://doi.org/10.1002/jbm.820250708
12. Anselme K. Osteoblast adhesion on biomaterials. Biomaterials 2000, 21, 667–681, https://doi.org/10.1016/s0142-9612(99)00242-2
13. Sul Y.T.; Johansson C.; Jeong Y.; Albrektsson T. The electrochemical oxide growth behaviour on titanium in acid and alkaline electrolytes. Med. Eng. Phys. 2001, 23, 329–346, https://doi.org/10.1016/s1350-4533(01)00050-9
14. Heimann R.B. Plasma-sprayed hydroxylapatite-based coatings. J. Therm. Spray Technol. 2016, 25, 827–850, https://doi.org/10.1007/s11666-016-0421-9
15. Dong H. Surface engineering of titanium alloys for biomedical applications. Surf. Eng. 2010, 26, 317–325.
16. Sun Y.; Bell T. Plasma surface engineering of titanium alloys for wear resistance. Surf. Coat. Technol. 1991, 49, 303–312.
17. Okuniewski W., Walczak M., Szala M., Chocyk D. Effect of surface modification by shot peening on cavitation erosion resistance of titanium alloy Ti-6Al-4V produced by DMLS method, Engineering Failure Analysis 2025; 176 https://doi.org/10.1016/j.engfailanal.2025.109653
18. Steen W.M.; Mazumder J. Laser Material Processing, 4th ed.; Springer: London, UK, 2010.
19. Dutta Majumdar J.; Manna I. Laser processing of materials. Sadhana 2003, 28, 495–562, https://doi.org/10.1007/BF02706446
20. Kurella A.; Dahotre N.B. Review paper: Surface modification for bioimplants. Mater. Sci. Eng. C 2005, 25, 815–823, https://doi.org/10.1177/0885328205052974
21. Ion J.C. Laser Processing of Engineering Materials; Butterworth-Heinemann: Oxford, UK, 2005, https://doi.org/10.1016/B978-075066079-2/50009-X
22. Mridha S.; Baker T.N. Laser surface melting of Ti–6Al–4V alloy. J. Mater. Process. Technol. 1997, 63, 432–438.
23. Majkowska-Marzec B., Jażdżewska M., Wołowiec E., Piekoszewski W., Klimek L., Zieliński A. The possibility of use of laser modified Ti6Al4V alloy in friction pairs in endoprostheses. Archives of Metallurgy and Materials. 2015, 16(2), 755–758, https://doi.org/10.1515/amm-2015-0202
24. Saleh A.F., Abboud J.H., Benyounis K.Y.,Surface carburizing of Ti–6Al–4V alloy by laser melting. Optics and Lasers in Engineering, 2010. 48, 257-267, https://doi.org/10.1016/j.optlaseng.2009.11.001
25. Guo B.; Zhou J.; Zhang S.; He J. Effect of laser surface melting on microstructure and wear resistance of Ti–6Al–4V alloy. Appl. Surf. Sci. 2011, 257, 8173–8179, https://doi.org/10.1016/S0921-5093(03)00519-7
26. Baufeld B.; Van der Biest O.; Gault R. Additive manufacturing of Ti–6Al–4V components by shaped metal deposition. Mater. Des. 2010, 31, S106–S111, https://doi.org/10.1016/j.matdes.2009.11.032
27. Majkowska-Marzec B.; Staszewski K.; Sypniewska J. Effect of pulse laser treatment at different process variables on mechanical behavior of carbon nanotubes electrophoretically deposited on titanium alloy. Acta of Bioengineering and Biomechanics. 2023, 25(2), 157–168, https://doi.org/10.37190/abb-02324-2023-02
28. Fadeeva E.; Truong V.K.; Stiesch M.; Chichkov B.N.; Crawford R.J.; Wang J.; Ivanova E.P. Bacterial retention on superhydrophobic titanium surfaces fabricated by femtosecond laser ablation. Langmuir 2011, 27, 3012–3019, https://doi.org/10.1021/la104607g
29. Rupp F.; Scheideler L.; Olshanska N.; de Wild M.; Wieland M.; Geis-Gerstorfer J. Enhancing surface free energy and hydrophilicity through chemical modification of microstructured titanium implant surfaces. J. Biomed. Mater. Res. A 2006, 76, 323–334, https://doi.org/10.1002/jbm.a.30518
30. Majkowska-Marzec B.; Tęczar P.; Bartmański M.; Bartosewicz B.; Jankiewicz B.J. Mechanical and Corrosion Properties of Laser Surface-Treated Ti13Nb13Zr Alloy with MWCNTs Coatings; Published: 9 September 2020; Materials, https://doi.org/10.3390/ma13183991.
31. Zieliński J.; Serbiński W.; Majkowska B.; Jażdżewska

M.; Skalski I. Influence of laser remelting at cryogenic conditions on corrosion resistance of non-ferrous alloys. Advances in Materials Science. 2009, 9(2), 21–28, https://doi.org/10.2478/v10077-009-0018-9

32. Sypniewska J.; Szkodo M.; Majkowska-Marzec B.; Mielewczyk-Gryń A. D. Exploring the composition and corrosion resistance in hybrid-modified Ti13Nb13Zr alloy. MRS Communications, October 2024, https://doi.org/10.1557/s43579-024-00663-z
33. Jażdżewska M.; Kwidzińska D. B.; Seyda W.; Frydrych D.; Zieliński A. Mechanical properties and residual stress measurements of grade IV titanium and Ti-6Al-4V and Ti-13Nb-13Zr titanium alloys after laser treatment. Materials October 2021, 14(21), 6316, https://doi.org/10.3390/ma14216316
34. Simoes I.G.; Candido dos Reis A.; Lima da Costa Valente M. Influence of surface treatment by laser irradiation on bacterial adhesion on surfaces of titanium implants and their alloys: Systematic review. Saudi Dental Journal 2023, 35, 111–124. https://doi.org/10.17605/OSF.IO/FTA3W
35. Das B.; Srivastava S.K.; Manna I.; Majumdar J.D. Mechanically tailored surface of titanium based alloy (Ti6Al4V) by laser surface treatment. Surface & Coatings Technology 2024, 479, 130560. https://doi.org/10.1016/j.surfcoat.2024.130560
36. Kwidzińska D.B.; Jażdżewska M.; Fydrych D. The influence of selected metal oxides and laser modification on the surfaces of titanium alloys – Bibliometric and systematic review. Optics & Laser Technology 2025, 184, 112592. https://doi.org/10.1016/j.optlastec.2025.112592
37. Mthisi A.; Popoola A.P.I.; Kanyanel R.; Raji S.A.; Malatji N. The possibility of using laser surface engineered titanium alloy implants as a treatment for cardiovascular diseases. Biomedical Engineering Advances 2024, 8, 100131. https://doi.org/10.1016/j.bea.2024.1001338.
38. Heinrich J.; Ränke F.; Schwarzenberger K.; Yang X.; Marzec M.M.; Sokołowski K.; Lasagni A.F.; Eckert K. Direct laser interference patterning for wettability modification and bubble nucleation on conventional and additively manufactured metals. Langmuir 2026, 42, 9951−9964. https://doi.org/10.1021/acs.langmuir.6c00056
39. Rafieea K.; Naffakh-Moosavya H.; Tamjid E. The effect of laser frequency on roughness, microstructure, cell viability and attachment of Ti6Al4V alloy. Materials Science & Engineering C 2020, 109, 110637.
40. Al-Aqeeli N., Yilbas B.S., Tabet N. The effect of laser pulse frequency on the microstructure and morphology of duplex treated Ti-6Al-4V alloy. Surface & Coatings Technology 2011, 205, 3073–3079. https://doi.org/10.1016/j.surfcoat.2010.11.024
41. Singh P.C.; Shukla V.K.; Singh R.K. Laser generated micro/nanotexturing and controllable wettability of the titanium surface for its implications in different fields. Optics & Laser Technology 2026, 198, 114938. https://doi.org/10.1016/j.optlastec.2026.114938
42. Ullah A.; Medvedev A.E.; Herzog D.; Molotnikov A.; Liu T.; Kelbassa I.; Brandt M. Role of laser beam shape and energy density in modulating surface quality, porosity, microstructure, and mechanical properties of PBF-LB/M Ti6Al4V. Journal of Materials Processing Tech. 2026, 348, 119197. https://doi.org/10.1016/j.jmatprotec.2026.119197
43. Praveenkumar K.; Vishnu J.; Raheem A.; Gopal V.; Swaroop S.; Suwas S.; Shankar B.; Manivasagam G. In-vitro fretting tribocorrosion and biocompatibility aspects of laser shock peened Ti6Al4V surfaces. Applied Surface Science 2024, 665, 160334. https://doi.org/10.1016/j.apsusc.2024.160334
44. Song S.; Meng Y.; Lv J.; Wang S.; Pan, Y.; Fu X.; Pan Y. Tailoring tribological properties of Ti6Al4V alloy via solution-assisted femtosecond laser texturing. Optics & Laser Technology 2026, 196, 114649. https://doi.org/10.1016/j.optlastec.2025.114649
45. Jażdżewska M.; Zieliński A. Laser-Enhanced Surface structurization of Titanium and Its alloys. [In] Surface Modifications of Titanium and Its alloys for Biomedical Applications, A. Zieliński, T. Moskalewicz and A.R. Boccaccini ([eds.],pp. 124-152 CRC Press, Bica Raton FL, USA, 2026, https://doi.org/10.1201/9781003527879-6
46. Jażdżewska M.; Majkowska-Marzec B.; Ostrowski R.; Olive J.M. Influence of surface laser treatment on mechanical properties and residual stresses of titanium and its alloys. Advances in Science and Technology Research Journal 2023, 17(6), 27–38. https://doi.org/10.12913/22998624/172981
47. Saurabh S.; Shaw P.K.; Dixit A.R.; Mandal D.K. Bio-inspired additive texturing of Ti6Al4V using laser powder bed fusion and its feasibility analysis for biomedical applications. Materials Today Communications 2026, 51, 114674. https://doi.org/10.1016/j.mtcomm.2026.114674
48. Kurek A.; Żrodowski Ł.; Choma T.; Abramczyk I.; Kłonica M.; Wachowski M. Enhancing fatigue performance of additively manufactured Ti6Al4V – The role of surface characteristics and post-processing techniques. Advances in Science and Technology Research Journal 2024, 18(6), 280–290. https://doi.org/10.12913/22998624/192114
49. Maruda R.W.; Leksycki K.; Wojciechowski S.; Feldshtein E.; Łukaszewicz A. Evaluation of the surface topography of Ti6Al4V alloy after the finish turning process under ecological conditions. Advances in Science and Technology Research Journal 2023, 17(2), 63–70. https://doi.org/10.12913/22998624/159801
50. Pfleging W.; Kumaria R.; Besserb H.; Scharnweberc

T.; Majumdara J.D. Laser surface textured titanium alloy (Ti–6Al–4V): Part 1 – Surface characterization. Applied Surface Science 2015, 355, 104–111. http://dx.doi.org/10.1016/j.apsusc.2015.06.175

51. Sypniewska J.; Szkodo M. Influence of laser modification on the surface character of biomaterials: Titanium and its alloys—a review. Coatings 2022, 12, 1371. https://doi.org/10.3390/coatings12101371
52. Wang Z.; Liu J.; Li K.; Fang X.; Wahab M.A.; Cai Z. Combined laser shock peening and shot peening for improving fretting wear and low-cycle fatigue performance of Ti6Al4V. Optics & Laser Technology 2026, 203, 115900.
53. Madapana D.; Ramadas H.; Nath A.K.; Majumdar J.D. Effect of laser shock peening parameters on electrochemical and tribocorrosion behaviour of Ti6Al4V alloy in simulated body fluid. Optics & Laser Technology 2026, 203, 115761. https://doi.org/10.1016/j.optlastec.2026.115761
54. Madapana D.; Bathe R.; Manna I.; Majumdar J.D. Laser surface structuring of titanium alloy (Ti-6Al-4V) for improved tribocorrosion resistance for bio-implant applications. Tribology International 2024, 197, 109711. https://doi.org/10.1016/j.triboint.2024.109711
55. Bera T.; Manna I.; Majumdar J.D. Laser-assisted microstructural engineering of near-beta titanium alloy (Ti-13Nb-13Zr) surface using fibre-coupled diode laser and its effect on wear and tribo-corrosion performance. Surface & Coatings Technology 2026, 521, 133097. https://doi.org/10.1016/j.surfcoat.2025.133097
56. Das B.; Srivastava S.K.; Manna I.; Majumdar J.D. Studies on kinetics and mechanism of tribo-corrosion of in situ laser composite surfaced Ti6Al4V using diode laser. Tribology International 2026; 214; 111042. https://doi.org/10.1016/j.triboint.2025.111042
57. David R.; Bannaravuri P.K.; Rao G.B.; Jestine C.; Joy R.; Masepogu W.K. Effects of fiber laser treatment on properties of Ti-64 alloy. Materials Today: Proceedings. Article in press. https://doi.org/10.1016/j.matpr.2023.10.060
58. Wang Y.; Bai H.; Yu Z.; Zhao J.; Hu J. Strategies for synergistic regulation of wear resistance, corrosion resistance, and antibacterial performance on implant surfaces. Colloids and Surfaces A: Physicochemical and Engineering Aspects 2026, 749, 141189. https://doi.org/10.1016/j.colsurfa.2026.141189